The Journal of Chemical Physics

Communication: State-to-state dynamics of the Cl + H_2O → HCl + OH reaction: Energy flow into reaction coordinate and transition-state control of product energy disposal

Cite as: J. Chem. Phys. **142**, 241101 (2015); https://doi.org/10.1063/1.4922650
Submitted: 20 May 2015 • Accepted: 05 June 2015 • Published Online: 22 June 2015

Bin Zhao, Zhigang Sun and Hua Guo

Communication: State-to-state dynamics of the Cl + H_2O → HCl + OH reaction: Energy flow into reaction coordinate and transition-state control of product energy disposal

Bin Zhao,[1] Zhigang Sun,[2] and Hua Guo[1,a)]
[1]*Department of Chemistry and Chemical Biology, University of New Mexico, Albuquerque, New Mexico 87131, USA*
[2]*Center for Theoretical and Computational Chemistry, and State Key Laboratory of Molecular Reaction Dynamics, Dalian Institute of Chemical Physics, Chinese Academy of Sciences, Dalian 116023, China*

(Received 20 May 2015; accepted 5 June 2015; published online 22 June 2015)

Quantum state-to-state dynamics of a prototypical four-atom reaction, namely, Cl + H_2O → HCl + OH, is investigated for the first time in full dimensionality using a transition-state wave packet method. The state-to-state reactivity and its dependence on the reactant internal excitations are analyzed and found to share many similarities both energetically and dynamically with the H + H_2O → H_2 + OH reaction. The strong enhancement of reactivity by the H_2O stretching vibrational excitations in both reactions is attributed to the favorable energy flow into the reaction coordinate near the transition state. On the other hand, the insensitivity of the product state distributions with regard to reactant internal excitation stems apparently from the transition-state control of product energy disposal. © *2015 AIP Publishing LLC.* [http://dx.doi.org/10.1063/1.4922650]

A central issue in chemistry is concerned with how chemical reactions are activated by various forms of energy.[1–3] The most effective way to overcome the reaction barrier is to channel energy into the reaction coordinate near the transition state. However, as the definition of the reaction coordinate changes as the reaction progresses, it is not always clear which of the reactant mode is the most effective in this respect. As a result, a better understanding of the dependence of reactivity on reactant mode excitation, namely, mode specificity, is highly desired. Much work has been done in this direction, particularly for gas-phase bimolecular reactions.[1–5] Sometime ago, Polanyi proposed two empirical rules concerning the mode specificity in atom-diatom reactions.[6] For a reaction with an early barrier, translational energy is more effective than the same amount of vibrational energy in surmounting the barrier and vice versa for a reaction with a late barrier. Invoking microscopic reversibility, these intuitive rules also predict product energy disposal. While they have guided our understanding of mode specificity, these venerable rules are difficult to extend to reactions with polyatomic reactants. In the title reaction, for example, there are three vibrational modes in H_2O and their efficacies in promoting the reactivity are likely to be different.

It is important to note that Polanyi recognized the paramount importance of the transition state in reaction dynamics by using the location of the barrier as a key descriptor for the relative efficacy of the vibrational and translational modes in promoting the reaction. Recently, we have generalized Polanyi's rules to polyatomic reactions by introducing the Sudden Vector Projection (SVP) model,[7–10] which attributes the ability of a reactant mode in promoting the reaction to the projection of the corresponding normal mode onto the reaction coordinate at the transition state. In the sudden limit, energy flow into the reaction coordinate at the transition state, which dictates the ability to overcome the barrier, is largely determined by how the vector of the reactant mode is aligned with it. The excitation in the product modes can be predicted analogously by invoking microscopic reversibility. Like the Polanyi rules, the SVP model also assigns a key role to the transition state, although with a more quantitative measure replacing the location of the barrier as the descriptor. We have recently studied the X + H_2O → HX + OH (X = F, Cl, O(^{3}P)) reactions systematically on accurate full-dimensional potential energy surfaces (PESs) and these studies have shown that the mode specificity and related bond selectivity can be largely understood in terms of the SVP model.[5]

In this Communication, we address the question on how reactant excitations influence product state distributions. Such state-to-state mode specificity has seldom been addressed quantum mechanically for reactions involving polyatomic reactants, because of the difficulties associated with quantum state-to-state calculations. Full-dimensional quantum state-to-state dynamical studies beyond triatomic reactions have only been reported for the H + H_2O,[11–16] HO + CO,[17,18] F + H_2O,[19] and H + CH_4 reactions.[20] Here, we present the first full-dimensional quantum study of the state-to-state reaction dynamics for the title reaction at total angular momentum $J = 0$. This reaction and its reverse are of great importance in atmospheric chemistry[21] and have also served as a prototype for understanding mode specificity in reaction dynamics.[1,5] Experimental studies found that the excitation of the local OH bond to $v_{OH} = 4$ in HOD enhances the O–H cleavage by eightfold,[22] and the released energy is mostly deposited into the internal excitation of the HCl product with internally cold OD.[23] These results suggest that the non-reactive OD moiety serves essentially as a spectator. Very recently, we

a)Author to whom correspondence should be addressed. Electronic mail: hguo@unm.edu

have reported quasi-classical trajectory (QCT) and initial state specific quantum dynamical (QD) calculations of the title reaction and its reverse using a recently developed global PES based on *ab initio* calculations.[24–28]

The state-to-state quantum dynamical calculations reported here are made possible using a transition-state wave packet (TSWP) method recently proposed by Manthe and coworkers,[29–31] which is an extension of Miller's quantum transition-state theory.[32,33] Our implementation of this method has been discussed in detail elsewhere,[16,34] so only a brief outline is given here. Specifically, the initial TSWPs are defined in the transition-state region as the eigenstates ($|f_T^n\rangle$) of the thermal flux operator:[35] $\hat{F}_T = e^{-\hat{H}/2k_BT}\hat{F}e^{-\hat{H}/2k_BT}$, where T is a reference temperature in Kelvin, $\hat{F}$ is the flux operator, and k_B denotes the Boltzmann constant. Dynamical information is then obtained by propagating these initial TSWPs into the asymptotic regions of both the reactant and product channels. The S-matrix element for a transition from an initial reactant state i to a final product state f is thus obtained by

$$S_{f\leftarrow i}(E) = \frac{\langle \Phi_f^- | \delta(\hat{H}-E) | \Phi_i^+ \rangle}{\Phi_f^{+*}(E)\eta_i^-(E)} = \frac{e^{E/k_BT}}{2\pi\eta_f^{+*}(E)\eta_i^-(E)} \sum_n f_T^n A_{f\leftarrow n}(E) A_{n\leftarrow i}^*(E), \quad (1)$$

where $\eta_i^-(E)$ and $\eta_f^+(E)$ are the energy normalization factors for the asymptotic reactant and product states, $|\Phi_i^-\rangle$ and $|\Phi_f^+\rangle$, respectively, and f_T^n are the eigenvalues of the thermal flux operator. The energy-resolved projection amplitudes, $A_{f\leftarrow n}(E)$ and $A_{n\leftarrow i}^*(E)$, are given as Fourier transforms of the appropriate cross-correlation functions by propagating the TSWPs into both the reactant and product arrangement channels,

$$A_{f\leftarrow n} = \int_{-\infty}^{\infty} dt e^{iEt} C_{f\leftarrow n}(t) = \int_{-\infty}^{\infty} dt e^{iEt} \langle \Phi_f^+ | e^{-i\hat{H}t} | f_T^n \rangle, \quad (2a)$$

$$A_{n\leftarrow i}^* = \int_{-\infty}^{\infty} dt e^{-iEt} C_{n\leftarrow i}^*(t) = \int_{-\infty}^{\infty} dt e^{-iEt} \langle f_T^n | e^{i\hat{H}t} | \Phi_i^- \rangle. \quad (2b)$$

More details of the theory and implementation are given in the supplementary material.[36]

The aforementioned TSWP approach has several unique advantages. First, the propagations are essentially of the inelastic type, within one set of scattering coordinates. This is important because it alleviates the "coordinate problem" in state-to-state scattering calculations.[37] Coordinate transformation is still needed, but only performed once at the beginning of the propagation. Further efficiency can be gained by parallel propagations of the TSWPs. Finally, the formulation based on the thermal flux eigenstates allows a straightforward analysis of the role of the transition state in influencing reaction dynamics.[30]

In Fig. 1, the reaction path profile of the title reaction (R1) is compared with that of the H + H_2O → H_2 + OH reaction (R2). The latter has been studied using the same TSWP method in our earlier work.[16] It is thus profitable to compare at the state-to-state level the behavior of these two endoergic reactions, which have very similar characteristics in reaction energy, barrier location, and barrier height. In the same figure, thermal

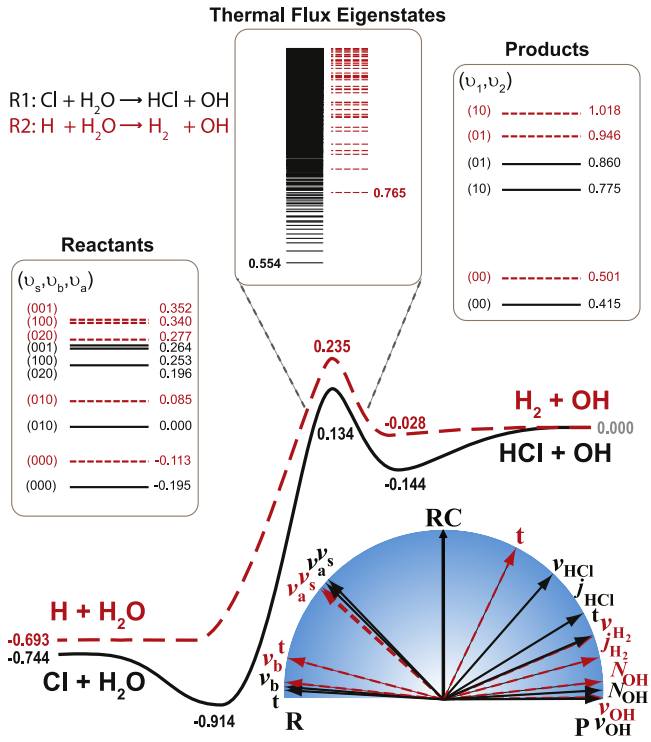

FIG. 1. Energetics (eV) of the Cl + H_2O → HCl + OH reaction (R1) in comparison with that of the H + H_2O → H_2 + OH reaction (R2). The energy is relative to the product asymptotes. (υ_s, υ_b, and υ_a) denote the vibrational quantum numbers of the symmetric stretching, bending, and antisymmetric stretching modes of H_2O, respectively, and (υ_1 and υ_2) denote the vibrational quantum numbers of HCl/H_2 and OH, respectively. The alignment of reactant/product vectors with the reaction coordinate at the transition state is also shown.

flux eigenenergies are also displayed for both reactions. The thermal flux eigenenergies are defined relative to the zero-point energy (E_{ZPE}) of the activated complex as $E_n \approx -k_BT(\ln f_T^n - \ln f_T^0) + E_{ZPE}$. It is clear from the figure that the density of thermal flux eigenstates for R1 is much higher than that for R2, due mainly to the heavier atomic mass of Cl atom. In our calculations, 400 pairs of such states were used, which made the calculations much more intense than those for R2. As discussed above, the thermal flux eigenstates were propagated separately into the reactant and product asymptotic regions and projected onto the asymptotic states to obtain the correlation functions in Eq. (2). The presence of the pre- and post-reaction wells in the reaction path of R1 does not seem to cause much numerical difficulties, as long as the dividing surface (flux operator) avoids the wells. These wells could conceivably make other state-to-state approaches, such as reactant-product decoupling (RPD),[38] more difficult to converge due to recurrences. In the supplementary material,[36] the details of the calculations are provided.

It is well established that the non-reacting OH moiety is a spectator in both reactions, resulting in a vibrationally cold OH product.[5] As a result, we focus on the HCl or H_2 product with the OH product in its vibrational ground state. In Fig. 2, reaction probabilities are shown for both the ground and first excited vibrational channels of the HCl or H_2 product summed over their rotational populations. Overall, the reaction probabilities of R1 are about fourfold smaller than those of R2, consistent with previous studies.[24,25,28] At the energies studied,

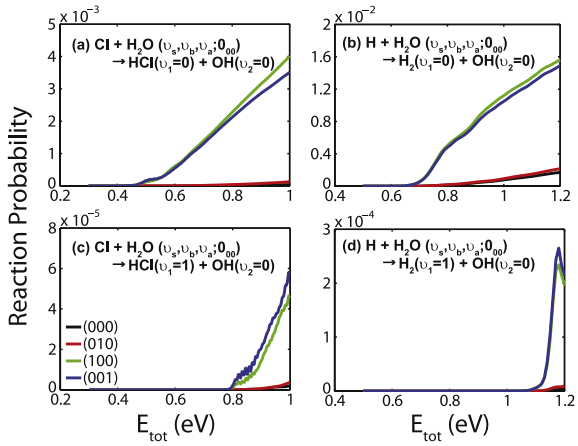

FIG. 2. Mode selectivity in product vibrational state resolved and rotational state summed state-to-state reaction probabilities for R1: (a) and (c) and R2: (b) and (d). OH is in the ground vibrational state, while the co-product HCl/H_2 is either in the ground vibrational state: (a) and (b) or the first excited vibrational state: (c) and (d).

the HCl and H_2 products are mostly in their ground vibrational states with the excited state populations about two orders of magnitude smaller. (The peak in the $H_2(v = 1)$ channel is likely due to a resonance, which will be analyzed in future work.) The reaction threshold for R1 is about 0.2 eV higher than that for R2, due presumably to the higher adiabatic barrier of R1, as suggested in Fig. 1. The most striking feature of these results is that the excitations of the H_2O stretching modes greatly enhance the reaction, while the bending mode excitation has a negligible effect. In addition, the efficacies of the symmetric and antisymmetric stretching modes are quite similar, and both are larger than that for translation. These observations are consistent with our earlier initial state specific QD study[28] as well as state-to-state QCT results,[25,26] in terms of the mode specificity.

The large enhancement of reactivity by the reactant stretching vibrations is consistent with a naïve extension of Polanyi's rules and can also be attributed to their strong coupling with the reaction coordinate at the transition state, according to the SVP model.[8] As shown in Fig. 1, the projection of the two H_2O stretching modes onto the reaction coordinate is quite large for both R1 and R2. This suggests that energy deposited into these reactant modes flows favorably into the reaction coordinate in the activated complex. For the bending and translational modes, on the other hand, the projections are relatively small and consequently, only a small portion of the energy deposited into these modes can be utilized to overcome the barrier. The confirmation of the SVP predictions by our QD results implies that the reaction indeed proceeds in the sudden limit, and the energy flow to the reaction coordinate occurs only near the transition state.

A natural question next is whether the strong mode specificity noted above has any influence on the product state distribution. In Fig. 3, the rotational state distributions of HCl/H_2 and OH products in their respective ground vibrational states are plotted for both the R1 and R2 reactions at a total energy of 0.5 eV above the zero-point energy of final products. The two reactions have different rotational state distributions, which is natural as they have different PESs and kinematics. The rotational state distributions of the two products are also highly correlated, with a colder OH distribution. Interestingly though, the product rotational state distributions in each reaction are rather insensitive to the reactant vibrational levels. This is more clearly demonstrated in the product energy decomposition shown in Fig. S4 of the supplementary material.[36] It is also quite clear in Fig. 2 that the relative reactivities of the H_2/HCl $v = 1$ and $v = 0$ channels are essentially unchanged whether or not the reactant vibrational modes are excited. In addition, it is shown in the supplementary material[36] that rotational excitations of H_2O have also a limited impact on the product state distributions. It can thus be concluded that while initial excitations of reactant modes have a significant effect on the overall reactivity, they have little influence on the product state distributions, at least at the energies studied here. This "loss of memory" phenomenon is very similar to that recently observed in the $H + CH_4 \rightarrow H_2 + CH_3$ reaction.[20]

The lack of correlation between product state distributions and initial reactant excitations in these prototypical reactions suggests that the product energy disposal is mainly controlled by the transition state. To confirm this, it is instructive to consider the SVP model again, which argues that in the sudden limit, the product energy disposal is completely determined by the alignment of the product normal mode vectors with the reaction coordinate at the transition state. As shown in Fig. 1, the rotational mode of H_2 or HCl has a stronger coupling with the reaction coordinate at the transition state than the OH rotation, consistent with the rotational state distributions in Fig. 3. Indeed, the rotation of HCl is more highly excited than H_2 because of its larger SVP value. The SVP model also predicts minimal excitation in the internal degrees of freedom of the OH product. On the other hand, the maximal energy studied in this work is only slightly higher than the $v = 1$ states for H_2 and HCl, and as a result, only a small population in the vibrationally excited states is present, despite the fact that the SVP model predicts that the H_2/HCl vibrations have significant overlaps with the corresponding reaction coordinates. At higher energies, however, it is expected that excited vibrational levels of these two products will have larger populations. Indeed, an experimental study of the Cl + HOD ($v_{OH} = 4$) reaction has observed significant HCl internal excitation[23] and our theoretical studies have also shown that the vibrationally excited HCl promotes the reverse HCl + OH reaction.[27] The consistency of our results with the SVP predictions supports the notion that the product state distributions are largely dictated by the transition state. We note that this sudden idea has in the past been used by many to obtain approximate product state distributions.[39–43]

Finally, we note that a large number of TSWPs contribute to each specific state-to-state reaction probability, and more TSWPs are typically needed to converge the reaction probabilities at higher energies. This is not surprising as the thermal flux eigenstates form a coherent (and complete) basis set to represent the activated complex and the number of such basis functions increases with energy. Our calculations found no domination of any single TSWP in any of the state-to-state reaction probabilities, although significant interferences are noted, as in the case of the $F + H_2O \leftrightarrow HF + OH$ reaction.[19]

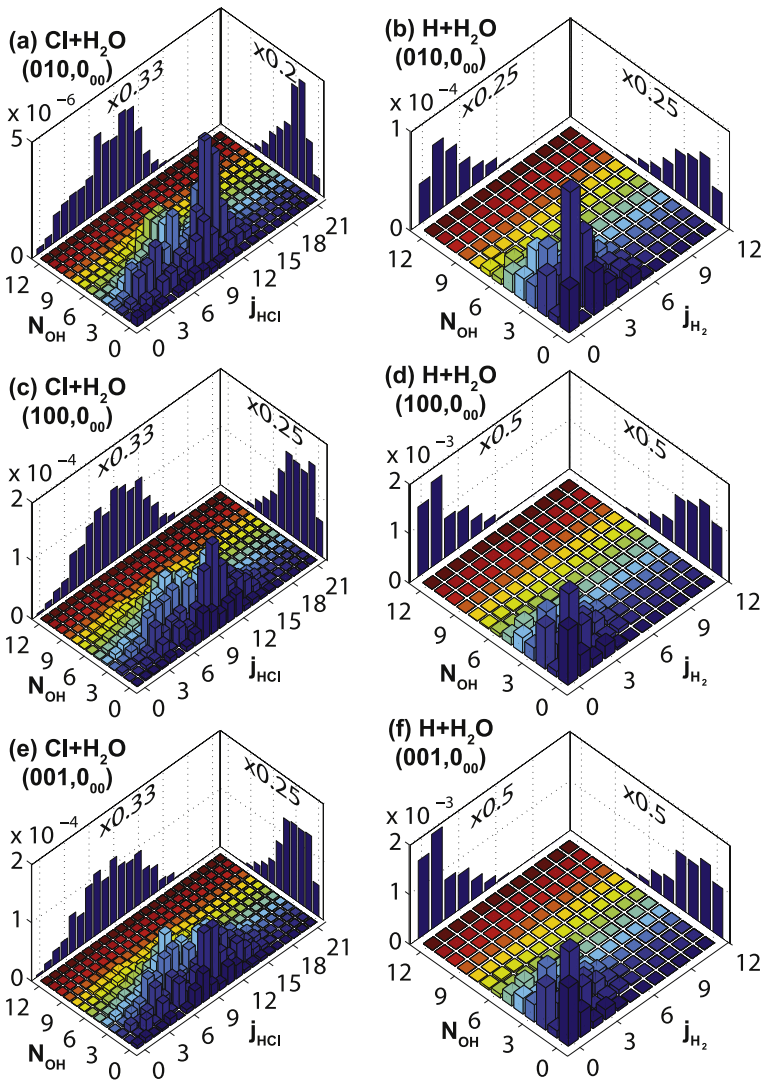

FIG. 3. Rotational state distributions of HCl/H_2 and OH products in R1 reaction: (a), (c), and (e) and R2 reaction: (b), (d), and (f). The rotationless H_2O is initially prepared in the bending mode (010): (a) and (b), symmetric stretching mode (100): (c) and (d), and antisymmetric stretching mode (001): (e) and (f). The energy is chosen to be 0.5 eV above the ZPE of the final products, i.e., $E_{tot} = 0.915$ and 1.001 eV for R1 and R2 reactions, respectively, relative to the respective product asymptotic potential. Rotational state distributions of HCl/H_2 or OH are projected to the side wall by summing the rotational states of the co-product. Note that the quantum number N is used for the OH fragment, but ignoring the $^1/_2$ spin.

To summarize, the picture emerges from these quantum state-to-state results reported in this work depicts a two-step process for the reactions. The initial step is to surmount the reaction barrier, in which a sufficient amount of energy needs be channeled into the reaction coordinate at the transition state. For the two reactions studied here, the most effective way is to impart energy into the H_2O stretching modes, which facilitates favorable energy flow into the reaction coordinate. The second step involves the decomposition of the transient activated complex, in which the product energy disposal is largely determined by the alignment of the product normal mode vectors with the reaction coordinate at the transition state. Such a two-step view is consistent with the well-known Franck-Condon models for reactive scattering,[44–46] in which the state-to-state dynamical information can be approximately extracted from the overlaps between asymptotic wavefunctions and those at the transition state. These insights reaffirm the paramount importance of the reaction transition state in not only kinetics but also state-to-state dynamics.

The work at UNM is supported by U.S. Department of Energy (Grant No. DF-FG02-05ER15694) and the calculations are performed at the National Energy Research Scientific Computing (NERSC) Center. Z.S. acknowledges the National Natural Science Foundation of China (NNSFC) (Grant Nos. 21222308 and 21133006).

[1]F. F. Crim, Acc. Chem. Res. **32**, 877–884 (1999).
[2]F. F. Crim, Proc. Natl. Acad. Sci. U. S. A. **105**, 12654–12661 (2008).
[3]K. Liu, J. Chem. Phys. **142**, 080901 (2015).
[4]G. Czakó and J. M. Bowman, J. Phys. Chem. A **118**, 2839–2864 (2014).
[5]J. Li, B. Jiang, H. Song, J. Ma, B. Zhao, R. Dawes, and H. Guo, J. Phys. Chem. A **119**, 4667–4687 (2015).
[6]J. C. Polanyi, Acc. Chem. Res. **5**, 161–168 (1972).
[7]B. Jiang and H. Guo, J. Chem. Phys. **138**, 234104 (2013).
[8]B. Jiang and H. Guo, J. Am. Chem. Soc. **135**, 15251–15256 (2013).
[9]H. Guo and B. Jiang, Acc. Chem. Res. **47**, 3679–3685 (2014).
[10]B. Jiang, J. Li, and H. Guo, J. Chem. Phys. **140**, 034112 (2014).
[11]D. H. Zhang, J. Chem. Phys. **125**, 133102 (2006).
[12]M. T. Cvitaš and S. C. Althorpe, J. Chem. Phys. **134**, 024309 (2011).
[13]C. Xiao, X. Xu, S. Liu, T. Wang, W. Dong, T. Yang, Z. Sun, D. Dai, X. Xu, D. H. Zhang, and X. Yang, Science **333**, 440–442 (2011).
[14]S. Liu, X. Xu, and D. H. Zhang, J. Chem. Phys. **136**(14), 144302 (2012).
[15]M. T. Cvitaš and S. C. Althorpe, J. Chem. Phys. **139**(6), 064307 (2013).
[16]B. Zhao, Z. Sun, and H. Guo, J. Chem. Phys. **141**(15), 154112 (2014).
[17]S. Liu, X. Xu, and D. H. Zhang, J. Chem. Phys. **135**, 141108 (2011).
[18]S. Liu, J. Chen, B. Fu, and D. H. Zhang, Theor. Chem. Acc. **133**(10), 1558 (2014).
[19]B. Zhao and H. Guo, J. Phys. Chem. Lett. **6**, 676–680 (2015).
[20]R. Welsch and U. Manthe, J. Phys. Chem. Lett. **6**, 338–342 (2015).
[21]M. J. Molina, L. T. Molina, and C. A. Smith, Int. J. Chem. Kinet. **16**(9), 1151–1160 (1984).
[22]A. Sinha, J. D. Thoemke, and F. F. Crim, J. Chem. Phys. **96**, 372–376 (1992).

[23]J. D. Thoemke, J. M. Pfeiffer, R. B. Metz, and F. F. Crim, J. Phys. Chem. **99**(37), 13748–13754 (1995).
[24]J. Li, R. Dawes, and H. Guo, J. Chem. Phys. **139**, 074302 (2013).
[25]J. Li, H. Song, and H. Guo, Phys. Chem. Chem. Phys. **17**, 4259–4267 (2015).
[26]J. Li, J. C. Corchado, J. Espinosa-García, and H. Guo, J. Chem. Phys. **142**, 084314 (2015).
[27]H. Song and H. Guo, J. Phys. Chem. A **119**, 826–831 (2015).
[28]H. Song and H. Guo, J. Phys. Chem. A **119**, 6188–6194 (2015).
[29]R. Welsch, F. Huarte-Larrañaga, and U. Manthe, J. Chem. Phys. **136**, 064117 (2012).
[30]R. Welsch and U. Manthe, Mol. Phys. **110**, 703–715 (2012).
[31]U. Manthe and R. Welsch, J. Chem. Phys. **140**(24), 244113 (2014).
[32]W. H. Miller, J. Chem. Phys. **61**, 1823–1834 (1974).
[33]W. H. Miller, S. D. Schwartz, and J. W. Tromp, J. Chem. Phys. **79**, 4889–4899 (1983).
[34]B. Zhao, Z. Sun, and H. Guo, J. Chem. Phys. **140**(23), 234110 (2014).
[35]T. P. Park and J. C. Light, J. Chem. Phys. **88**, 4897–4912 (1988).
[36]See supplementary material at http://dx.doi.org/10.1063/1.4922650 for a brief discussion of the methods and numerical parameters used in our calculations.
[37]H. Guo, Int. Rev. Phys. Chem. **31**, 1–68 (2012).
[38]T. Peng and J. Z. H. Zhang, J. Chem. Phys. **105**, 6072–6074 (1996).
[39]M. J. Berry, Chem. Phys. Lett. **27**, 73–77 (1974).
[40]M. Bear, J. Chem. Phys. **60**, 1057–1063 (1974).
[41]D. C. Clary, J. Chem. Phys. **96**, 3656–3665 (1992).
[42]D. Wang and J. M. Bowman, Chem. Phys. Lett. **207**, 227–235 (1993).
[43]R. Schinke, *Photodissociation Dynamics* (Cambridge University Press, Cambridge, 1993).
[44]G. C. Schatz and J. Ross, J. Chem. Phys. **66**, 1021–1036 (1977).
[45]M. Gustafsson and R. T. Skodje, J. Chem. Phys. **124**, 144311 (2006).
[46]R. Welsch and U. Manthe, J. Chem. Phys. **141**(5), 051102 (2014).